Large-scale imaging of subcellular calcium dynamics of cortical neurons with G-CaMP6-actin

Chiaki Kobayashi[a], Masamichi Ohkura[b], Junichi Nakai[b], Norio Matsuki[a], Yuji Ikegaya[a,c] and Takuya Sasaki[a]

Understanding the information processing performed by a single neuron requires the monitoring of physiological dynamics from a variety of subcellular compartments including dendrites and axons. In this study, we showed that the expression of a fusion protein, consisting of a Ca^{2+} indicator protein (G-CaMP6) and a cytoskeleton protein (actin), enabled large-scale recording of Ca^{2+} dynamics from hundreds of postsynaptic spines and presynaptic boutons in a cortical pyramidal cell. At dendritic spines, G-CaMP6-actin had the potential to detect localized Ca^{2+} activity triggered by subthreshold synaptic inputs. Back-propagating action potentials reliably induced Ca^{2+} fluorescent increases in all spines. At axonal boutons, G-CaMP6-actin reported action potential trains propagating along axonal collaterals. The detectability of G-CaMP6-actin should contribute toward a deeper understanding of neural network architecture and dynamics at the level of individual synapses. ***NeuroReport*** **25:501–506 © 2014 Wolters Kluwer Health | Lippincott Williams & Wilkins.**

NeuroReport 2014, **25**:501–506

Keywords: axon, calcium, imaging, spine, synapse

[a]Graduate School of Pharmaceutical Sciences, University of Tokyo, Tokyo, [b]Brain Science Institute, Saitama University, Saitama and [c]Center for Information and Neural Networks, Osaka, Japan

Correspondence to Takuya Sasaki, PhD, Graduate School of Pharmaceutical Sciences, University of Tokyo, Tokyo 113-0033, Japan
Tel: +81 3 5841 4781; fax: +81 3 5841 4786;
e-mail: t.sasaki.0224@gmail.com

Received 6 December 2013 **accepted** 8 January 2014

Introduction

Neurons in the cortex are not simple integrate-and-fire units, but transform spatially structured synaptic inputs and provide a range of nonlinear outputs through the local interactions in dendrites [1] and axons [2]. A series of recent evidence suggests that these subcellular mechanisms are likely to enhance the computational power of a single neuron.

Although the patch-clamp recording technique is used widely for direct examination of subcellular physiological dynamics [3], this recording is restricted to one or a few patched sites. Alternatively, a promising strategy for resolving this spatial limitation is Ca^{2+} imaging in which activity patterns of identified structures are optically measured as a change in Ca^{2+} fluorescence. It has, however, still been a technical challenge to introduce Ca^{2+} indicators into small subcellular compartments. Intracellular loading of chemically synthesized indicators by whole-cell recording requires tens of minutes to allow passive dye diffusion into distal subcellular structures [4].

In recent imaging strategies, genetically encoded Ca^{2+} indicators (GECIs) can be alternatives to chemically synthesized indicators [5,6]. One of the remarkable advantages of GECIs is that they can be targeted to specific cell classes and subcellular domains by linking to cell-type selective promoters or sequences. In addition, stable expression of GECIs allows long-term recording from the same cellular structures [7,8]. In a recent study, we have developed a novel GECI, termed G-CaMP6 [9] (note that this G-CaMP6 is a different variant from a series of GCaMP6 developed by Chen *et al.* [8]). This new sensor allows reliable detection of neuronal activity with larger fluorescence signals and higher temporal resolution than previous versions of G-CaMPs. Next, we fused G-CaMP6 with actin, a major cytoskeletal protein, to yield G-CaMP6-actin. In this study, we characterized the ability of G-CaMP6-actin to detect localized Ca^{2+} signals at dendritic spines and axonal boutons in cortical pyramidal cells. We show that G-CaMP6-actin can visualize the entire subcellular morphology at rest and detect Ca^{2+} signals at a single-synapse resolution.

Materials and methods

Animal ethics

Experiments were conducted with the approval of the animal experimental ethics committee at the University of Tokyo (approval number: 24-6) according to the University of Tokyo guidelines for the care and use of laboratory animals.

Cultured slice preparation

Hippocampal slice cultures were prepared from postnatal day 7 Wistar/ST rats (SLC). Briefly, rat pups were chilled and the brains were removed and horizontally cut into 300-μm-thick slices in aerated, ice-cold Gey's balanced salt solution supplemented with 25 mM glucose. Entorhino-hippocampal stumps were excised and cultivated on Omnipore membrane filters (JHWP02500; Millipore, Bedford, Massachusetts, USA) that were laid on plastic

0959-4965 © 2014 Wolters Kluwer Health | Lippincott Williams & Wilkins DOI: 10.1097/WNR.0000000000000126

O-ring disks [10]. The cultures were fed with 1 ml of 50% minimal essential medium, 25% Hanks' balanced salt solution, 25% horse serum, and antibiotics in a humidified incubator at 37°C in 5% CO_2 and were used for experiments on days 7 to 14 *in vitro*. The medium was changed every 3.5 days.

Single-cell electroporation

On days 3–5 *in vitro*, G-CaMP6-actin under the control of the CMV promoter was introduced into the neurons through targeted single-cell electroporation [9,11]. Briefly, borosilicate glass pipettes (tip resistance, 4–6 MΩ) were filled with HBSS containing 1–2 μg/μl of plasmid DNA. After the tip of the pipette was placed in close proximity to the soma, electroporation was performed with 50 rectangular pulses (–5 V, 0.5 ms duration) at a frequency of 50 Hz. Single-cell electroporation was applied sequentially to up to 10 cells using the same pipette within 5 min. Imaging was performed 24–48 h after electroporation.

Ca^{2+} imaging

Hippocampal slices were mounted in a recording chamber and perfused at a rate of 1.5–3 ml/min with artificial cerebrospinal fluid containing (in mM) 127 NaCl, 26 $NaHCO_3$, 3.3 KCl, 1.24 KH_2PO_4, 2.2 $MgSO_4$, 2.4 $CaCl_2$, and 10 glucose, bubbled with 95% O_2 and 5% CO_2. All recordings were performed at room temperature (24–28°C). An epifluorescence microscope was used to select cells showing stable G-CaMP6-actin expression. For Ca^{2+} imaging, G-CaMP6-actin were excited at 488 nm with a laser diode (641-YB-A01; Melles Griot, Carlsbad, California, USA) and visualized using a 507 nm long-pass emission filter. Images were captured at 10–100 fps using a Nipkow-disk confocal scanner unit (CSU-X1; Yokogawa Electric, Tokyo, Japan), a cooled CCD camera (iXON DV897; Andor, Belfast, UK), an upright microscope (Eclipse FN1; Nikon, Tokyo, Japan), and a water-immersion objective (× 40, 0.9 NA; Nikon) [12,13]. Cells with labeled nuclei were excluded from further analysis. Regions of interest were carefully located by eye. In each region of interest, the fluorescence intensity was spatially averaged. The fluorescence change was defined as:

$$\frac{\Delta F}{F} = \frac{(F_t - F_0)}{F_0},$$

where F_t is the fluorescence intensity at time t and F_0 is the baseline averaged for 5 s before time t.

Electrophysiological recordings

Patch-clamp recordings were collected from hippocampal CA3 pyramidal neurons using a MultiClamp 700B amplifier and a Digidata 1440A digitizer controlled by pCLAMP10 software (Molecular Devices, Union City, California, USA). Borosilicate glass pipettes (5–7 MΩ) were filled with a solution containing (in mM) 135 K-gluconate, 4 KCl, 10 HEPES, 10 phosphocreatine-Na_2, 0.3 Na_2-GTP, and 4 Mg-ATP (pH 7.2). The signals were low-pass filtered at 1–2 kHz and digitized at 20 kHz. Data were discarded if the access resistance changed by more than 20% during the experiment. Spikes were evoked by current injections (2–3 ms, 1–2 nA). Extracellular electrical stimulation was applied using a constant voltage-isolated stimulator (Nihon Kohden) with a glass pipette filled with artificial cerebrospinal fluid. The electrodes were placed on the dentate hilus to stimulate the mossy fiber pathways. Stimulation intensity was set to 40–60 μA and greater than 200 μA for subthreshold and suprathreshold stimulation, respectively.

Results

Expression of G-CaMP6-actin in hippocampal pyramidal neurons

We have recently developed a GECI, termed G-CaMP6, which generates relatively higher baseline fluorescence compared with the existing GECIs and enables detection of individual spikes from the pyramidal cell soma with 100% detection rates in slice preparations [9]. Although the name of the probe is similar, this probe was developed independently from the study of GCaMP6f, m, and s reported by Chen *et al.* [8]. We then constructed a fusion protein in which G-CaMP6 is tethered to a cytoskeleton protein, actin, to localize the probe to plasma membranes of small subcellular compartments [14]. The resulting indicator, G-CaMP6-actin, was expressed in hippocampal pyramidal neurons through targeted single-cell electroporation of the cDNA plasmid (Fig. 1) [9,15]. G-CaMP6-actin labeled dendritic spines and axonal varicosities that represent excitatory synaptic inputs and outputs, respectively (Fig. 1a). No significant differences were found between G-CaMP6-actin(–) and G-CaMP6-actin(+) cell groups in membrane capacitances [G-CaMP6(–)-actin, 162 ± 49 pF; G-CaMP6-actin(+), 172 ± 29 pF] and input resistances [G-CaMP6(–)-actin, 128 ± 38 MΩ; G-CaMP6-actin(+), 130 ± 13 MΩ], indicating that tethering G-CaMP6 to actin and its expression did not alter the basic electrophysiological properties.

Imaging of spine Ca^{2+} activity with G-CaMP6-actin

In G-CaMP6-actin-expressing neurons, the density of labeled spines was 1.13 ± 0.98/μm ($n = 600$ spines from five cells), which was anatomically characterized spine densities reported in previous studies [16,17]. G-CaMP6-expressing spines in the striatum lucidum and the striatum radiatum of the hippocampal CA3 region were imaged using a Nipkow-disk confocal system for high-speed and wide-field scanning of Ca^{2+} dynamics from a large number of spines [12] (Fig. 1b). On average, spatiotemporal patterns of Ca^{2+} signals were reconstructed from 176 ± 44 spines ($n = 6$ movies) in an imaging region of $200 \times 200\ \mu m^2$. Field electrical stimulation was delivered to the dentate granule cell layer, and membrane potential changes were measured simultaneously by whole-cell recording from the imaged

Fig. 1

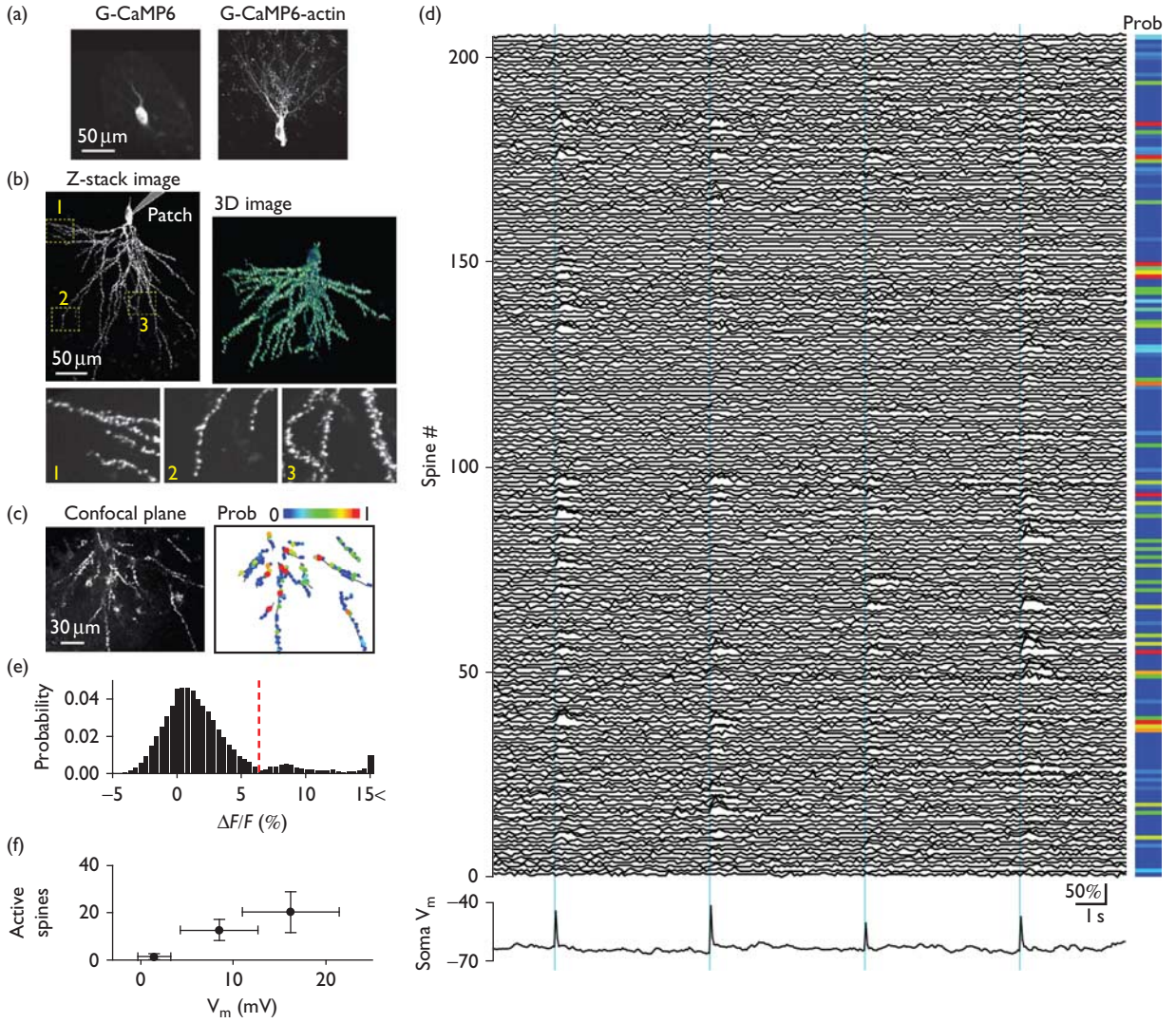

Imaging of spine signals associated with subthreshold activity. (a) Expression of G-CaMP6 (left) and G-CaMP6-actin (right) in hippocampal pyramidal neurons. The images were taken from different slices but under similar imaging conditions. Similar image processing was added to the pictures. (b) Z-projection and 3D images of a CA3 pyramidal neuron expressing G-CaMP6-actin obtained using a $\times 40$ objective. The bottom insets show the $\times 5$ magnification of the parts indicated by white boxes. (Right) Three-dimensional image reconstruction of the spines. (c) Confocal scanning was performed from the same neuron at a frame rate of 10–50 Hz. Ca^{2+} responses in spines were induced by a single pulse of subthreshold stimulation (0.2 Hz, 30–50 µV) to the dentate hilus. Membrane potential was recorded simultaneously from the soma by whole-cell recording. The positions of 206 spines are reconstructed in the right cell map, in which response probability of each spine is indicated in a pseudocolor scale. Out-of-focus portions of the dendrites are connected by black lines. (d) Representative fluorescent traces of the spines in response to the subthreshold stimulation imaged at a frame rate of 20 fps. Corresponding voltage response at the soma is shown in the bottom trace, indicating no spike generation. (e) The distribution of the maximum $\Delta F/F$ within 200 ms after the stimulation in all spines. The red line indicates the $\Delta F/F$ at the 1% significance level estimated from the Gaussian curve fit to the values obtained from inactive spines. (f) Relationship between the average amplitude of voltage changes and the percentage of active spines. Error bars represent SEM.

neuron. Corresponding with the timing of subthreshold voltage response, a subset of spines showed increases in Ca^{2+} fluorescence in an all-or-none manner (Fig. 1d). The spatial extent of the spine Ca^{2+} transients had an average radius of $2.3 \pm 0.8\,\mu m^2$ ($n = 85$ spines). Notably, individual spines showed trial-to-trial variations in Ca^{2+} responses; a few spines responded faithfully to the repetitive stimuli, whereas others were less reliable. Figure 1b and c shows the probability of a Ca^{2+} response (i.e. the ratio of the number of Ca^{2+} transients to the total trial of field stimulation). This value is likely to reflect the success rate of synaptic transmission at each spine. Amplitudes of $\Delta F/F$ transients in active trials were almost constant and the signals could be separated from optical noise at inactive trials or in spines that were functionally silent (Fig. 1e; $n = 4284$ responses). This suggests that the signal-to-noise ratio of G-CaMP6-actin

Fig. 2

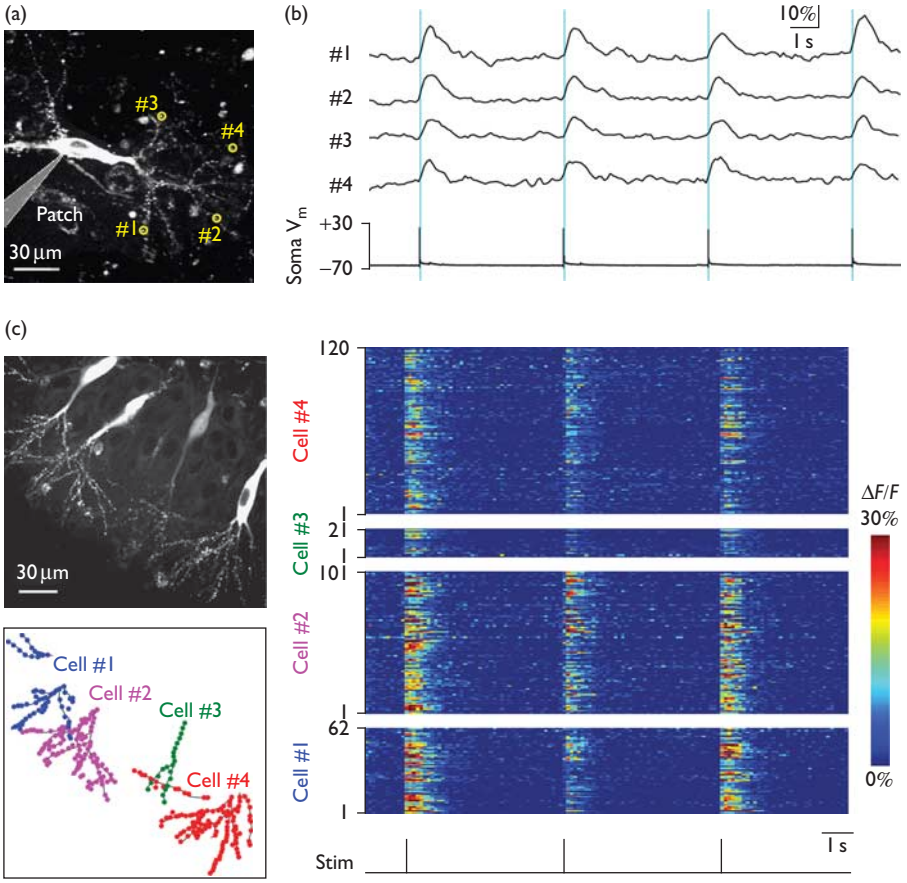

Imaging of spine Ca^{2+} transients triggered by back-propagating APs. (a) Typical changes in Ca^{2+} intensity were measured from the four spines of a G-CaMP6-actin-expressing cell indicated by yellow circles. (b) Representative fluorescent responses of four spines induced by spike generation at a frame rate of 10 fps. APs reliably induced a fast Ca^{2+} transient in all spines. (c) (Left) Simultaneous spine imaging from four G-CaMP6-actin-expressing neurons. Spines were numbered in ascending order from the soma to distal axonal segments in each cell. Out-of-focus portions are connected by black lines. (Right) Rastergraph showing the spike-induced Ca^{2+} transients of the 304 boutons from four pyramidal cells. The bottom shows the timing of suprathreshold electrical stimulation. APs, action potentials.

fluorescence is sufficient to detect spine Ca^{2+} signals at single trials. The average decay time constant of the Ca^{2+} signals was 556 ± 69 ms ($n = 1589$ responses). Overall, the fraction of active spines in each trial showed a significant positive correlation with the amplitude of subthreshold depolarization (Fig. 1f; $R = 0.75$; $P < 0.05$).

We next examined Ca^{2+} dynamics associated with suprathreshold activity by increasing the intensity of field stimulation to more than 200 µA. Patch-clamp recording confirmed that stimulation induced action potentials (APs) in all trials (Fig. 2b). Spike generation robustly induced fluorescence responses in $98.6 \pm 1.1\%$ of spines ($n = 6$ cells; an example shown in Fig. 2c). This result shows that G-CaMP6-actin faithfully captures spine Ca^{2+} influx induced by back-propagating APs into dendrites.

Imaging of axonal Ca^{2+} activity with G-CaMP6-actin

Because actin is a cytoskeleton protein distributed throughout axonal arbors, the expression of G-CaMP6-actin should also label presynaptic axonal boutons. In hippocampal pyramidal cells, axon collaterals can be distinguished from dendrites on the basis of their typical morphological characteristics: (a) axons are smaller in diameter than dendrites, (b) axons innervate wider areas with diverse directions, and (c) axons lack spiny structures. In G-CaMP6-actin expressing neurons, the average interval between boutons was 3.9 ± 2.2 µm ($n = 142$ boutons from four cells). This is consistent with the morphological characteristics of axons reported in previous studies [18]. We monitored Ca^{2+} responses upon spike generation from *en passant* boutons of axon collaterals with an axonal path distance of 100–300 µm from the axon hillock. Spike-triggered Ca^{2+} transients were restricted to bouton domains with minimal fluorescent changes in axonal shafts (Fig. 3b). The amplitudes of the bouton Ca^{2+} signals varied from trial to trial, which may be because of the intrabouton variations in spike-induced Ca^{2+} entry through voltage-sensitive Ca^{2+} channels as reported in previous studies [19]. The average $\Delta F/F$ amplitude of Ca^{2+} transients in response to a single spike was $9.4 \pm 2.6\%$,

Fig. 3

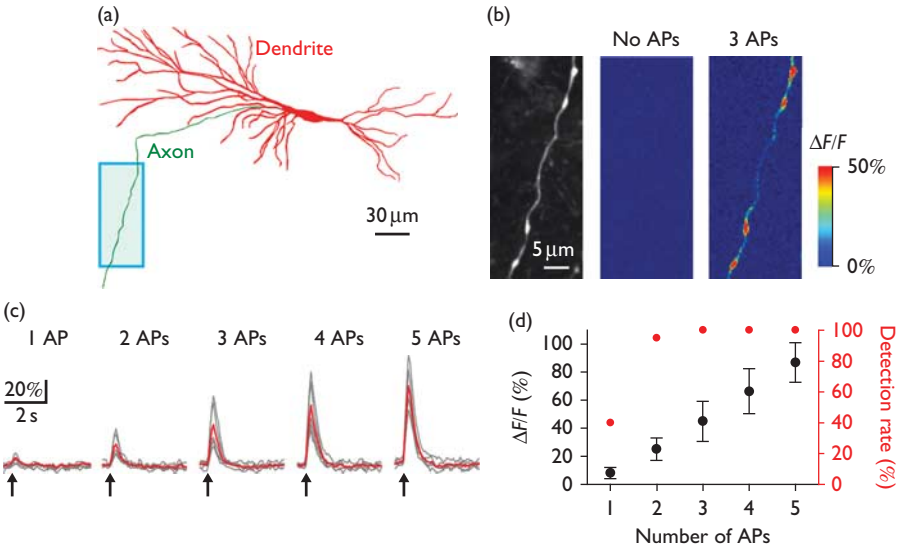

Imaging of spike-induced Ca^{2+} signals from presynaptic axonal boutons. (a) Axonal (green) and dendritic (red) trajectories reconstructed from a G-CaMP6-actin-expressing pyramidal cell. Imaging was carried out from axonal *en passant* boutons 150–200 µm apart from the soma at a frame rate of 10 fps. The imaging region shown in the rectangular window is magnified in (b) (left). (b) Pseudocolor $\Delta F/F$ images of axonal boutons with no APs (middle) and 3 APs (right). (c) Representative $\Delta F/F$ traces of axonal boutons in response to 1–5 APs induced at 50 Hz. Gray lines indicate traces recorded from five different boutons, on which the averaged traces are superimposed as thick red lines. (d) Average $\Delta F/F$ response (black) and detection rate of Ca^{2+} signals (red) plotted against the number of APs ($n=15$ boutons). APs, action potentials.

with a detection rate of 45% ($n = 15$ boutons). The signal amplitudes increased almost linearly as the spike number increased, and no apparent failures of Ca^{2+} responses were observed with two and more APs with a frequency of 50 Hz. The decay time constant of the axonal Ca^{2+} signals was 526 ± 48 ms.

Discussion

In this study, we showed that a fusion protein, G-CaMP6-actin, enables functional imaging of the spatiotemporal patterns of Ca^{2+} signals from a large number of subcellular domains in cortical pyramidal cells. G-CaMP6-actin can be a powerful tool to elucidate the spatiotemporal patterns of synaptic inputs and outputs in a single neuron.

The idea of creating a fusion protein composed of a GECI and actin was proposed by Mao *et al.* [14] as GCaMP2-actin. Owing to the iterative improvements of the sensor domain, our G-CaMP6-actin considerably outperforms the previous fusion protein to detect subcellular calcium transients, which are practically difficult to detect. Although it has been shown that the expression of raw GECIs labels dendrites and spines using certain expression systems [8], linking actin to GECIs can be another strategy to effectively target tiny subcellular domains as shown in Fig. 1a.

Individual spines responded to constant subthreshold inputs with considerable variations both among different spines at a given trial and among trials in a given spine. This could not be because of the instability of sensor performance because back-propagating APs triggered robust Ca^{2+} increases in every trial and in almost all spines. Several possible mechanisms may account for the response variability. First, the variation observed may reflect the instability of synaptic transmission. Neurotransmitter release from cortical synapses is stochastic and varies from trial to trial. Assuming that Ca^{2+} increase at each spine is linked to neurotransmission, the probability of Ca^{2+} response could directly report the success rate of transmission [20]. Second, the response variation might be because of the variability of individual Ca^{2+} dynamics triggered by synaptic transmission. Finally, the most likely source is time-varying recruitment of different subsets of presynaptic inputs that are determined by background noise activity arising from recurrent circuits of the hippocampal CA3 region.

The dominant source of spine Ca^{2+} influx is considered to be from the opening of voltage-dependent Ca^{2+} channels (VDCCs) in the plasma membrane triggered by back-propagating APs [19]. In addition to VDCCs, activation of *N*-methyl-D-aspartate receptors underlies Ca^{2+} transients associated with subthreshold depolarization induced by synaptic inputs [12,20,21]. At axonal boutons, spike-induced Ca^{2+} transients are controlled by activation of a high density of VDCCs at presynaptic terminals [22]. Another possible source might be *N*-methyl-D-aspartate receptors at presynaptic sites, although the distribution

and the possible contribution to axonal Ca^{2+} dynamics remain fully understood [23,24].

Here, we chose actin as a protein to fuse with GECIs simply because it is ubiquitously expressed throughout neurons. However, other types of fusion proteins or promoters may also be effective in localizing GECIs to targeted domains [25]. As the dynamics of GECIs strongly depend on external conditions, such as temperature, background fluorescent intensity, and expression systems, further studies are required to determine whether similar performance can be obtained in other experimental systems.

Acknowledgements

This work was partly supported by Grants-in-Aid for Science Research on Innovative Areas, 'Mesoscopic Neurocircuitry' (No. 22115003), from the Ministry of Education, Culture, Sports, Science and Technology of Japan and by the Funding Program for Next Generation World-Leading Researchers (LS023).

Conflicts of interest

There are no conflicts of interest.

References

1 Branco T, Hausser M. The single dendritic branch as a fundamental functional unit in the nervous system. *Curr Opin Neurobiol* 2010; **20**:494–502.
2 Debanne D. Information processing in the axon. *Nat Rev Neurosci* 2004; **5**:304–316.
3 Stuart GJ, Sakmann B. Active propagation of somatic action potentials into neocortical pyramidal cell dendrites. *Nature* 1994; **367**:69–72.
4 Chen X, Leischner U, Rochefort NL, Nelken I, Konnerth A. Functional mapping of single spines in cortical neurons in vivo. *Nature* 2011; **475**:501–505.
5 Palmer AE, Tsien RY. Measuring calcium signaling using genetically targetable fluorescent indicators. *Nat Protoc* 2006; **1**:1057–1065.
6 Kotlikoff MI. Genetically encoded Ca2+ indicators: using genetics and molecular design to understand complex physiology. *J Physiol* 2007; **578**:55–67.
7 Tian L, Hires SA, Mao T, Huber D, Chiappe ME, Chalasani SH, *et al*. Imaging neural activity in worms, flies and mice with improved GCaMP calcium indicators. *Nat Methods* 2009; **6**:875–881.
8 Chen TW, Wardill TJ, Sun Y, Pulver SR, Renninger SL, Baohan A, *et al*. Ultrasensitive fluorescent proteins for imaging neuronal activity. *Nature* 2013; **499**:295–300.
9 Ohkura M, Sasaki T, Sadakari J, Gengyo-Ando K, Kagawa-Nagamura Y, Kobayashi C, *et al*. Genetically encoded green fluorescent ca(2+) indicators with improved detectability for neuronal Ca(2+) signals. *PLoS One* 2012; **7**:e51286.
10 Koyama R, Muramatsu R, Sasaki T, Kimura R, Ueyama C, Tamura M, *et al*. A low-cost method for brain slice cultures. *J Pharmacol Sci* 2007; **104**:191–194.
11 Judkewitz B, Rizzi M, Kitamura K, Hausser M. Targeted single-cell electroporation of mammalian neurons in vivo. *Nat Protoc* 2009; **4**:862–869.
12 Takahashi N, Kitamura K, Matsuo N, Mayford M, Kano M, Matsuki N, *et al*. Locally synchronized synaptic inputs. *Science* 2012; **335**:353–356.
13 Takahashi N, Oba S, Yukinawa N, Ujita S, Mizunuma M, Matsuki N, *et al*. High-speed multineuron calcium imaging using Nipkow-type confocal microscopy. *Curr Protoc Neurosci* 2011 [Epub ahead of print].
14 Mao T, O'Connor DH, Scheuss V, Nakai J, Svoboda K. Characterization and subcellular targeting of GCaMP-type genetically-encoded calcium indicators. *PLoS One* 2008; **3**:e1796.
15 Ohkura M, Sasaki T, Kobayashi C, Ikegaya Y, Nakai J. An improved genetically encoded red fluorescent Ca(2+) indicator for detecting optically evoked action potentials. *PLoS One* 2012; **7**:e39933.
16 Arellano JI, Benavides-Piccione R, Defelipe J, Yuste R. Ultrastructure of dendritic spines: correlation between synaptic and spine morphologies. *Front Neurosci* 2007; **1**:131–143.
17 Fu M, Yu X, Lu J, Zuo Y. Repetitive motor learning induces coordinated formation of clustered dendritic spines in vivo. *Nature* 2012; **483**:92–95.
18 Shepherd GM, Raastad M, Andersen P. General and variable features of varicosity spacing along unmyelinated axons in the hippocampus and cerebellum. *Proc Natl Acad Sci USA* 2002; **99**:6340–6345.
19 Markram H, Helm PJ, Sakmann B. Dendritic calcium transients evoked by single back-propagating action potentials in rat neocortical pyramidal neurons. *J Physiol* 1995; **485**:1–20.
20 Yuste R, Majewska A, Cash SS, Denk W. Mechanisms of calcium influx into hippocampal spines: heterogeneity among spines, coincidence detection by NMDA receptors, and optical quantal analysis. *J Neurosci* 1999; **19**:1976–1987.
21 Yasuda R, Nimchinsky EA, Scheuss V, Pologruto TA, Oertner TG, Sabatini BL, *et al*. Imaging calcium concentration dynamics in small neuronal compartments. *Sci STKE* 2004; **2004**:pl5.
22 Reid CA, Bekkers JM, Clements JD. Presynaptic Ca2+ channels: a functional patchwork. *Trends Neurosci* 2003; **26**:683–687.
23 McGuinness L, Taylor C, Taylor RD, Yau C, Langenhan T, Hart ML, *et al*. Presynaptic NMDARs in the hippocampus facilitate transmitter release at theta frequency. *Neuron* 2010; **68**:1109–1127.
24 Corlew R, Brasier DJ, Feldman DE, Philpot BD. Presynaptic NMDA receptors: newly appreciated roles in cortical synaptic function and plasticity. *Neuroscientist* 2008; **14**:609–625.
25 Dreosti E, Odermatt B, Dorostkar MM, Lagnado L. A genetically encoded reporter of synaptic activity in vivo. *Nat Methods* 2009; **6**:883–889.